Asian Research Journal of Mathematics

7(3): 1-14, 2017; Article no.ARJOM.37941
ISSN: 2456-477X

Joule Heating Effects of the Coupling Conduction on MHD Free Convection Flow along a Vertical Flat Plate with Heat Generation

Md. M. Alam[1], Md. Saddam Hossain[1], M. M. Parvez[1*] and M. A. Rahman[1]

[1]Department of Mathematics, Dhaka University of Engineering and Technology, Gazipur, Bangladesh.

Authors' contributions

This work was carried out in collaboration between all authors. Author MMA designed the study, performed the statistical analysis, wrote the protocol and wrote the first draft of the manuscript. Authors MSH and MMP managed the analyses of the study. Authors MMP and MAR managed the literature searches. All authors read and approved the final manuscript.

Article Information

DOI: 10.9734/ARJOM/2017/37941
Editor(s):
(1) Cenap Ozel, Mathematics, King Abdulaziz University, Saudi Arabia and Dokuz Eylul University, Turkey.
Reviewers:
(1) Sanjib Kumar Datta, University of Kalyani, India.
(2) John Abraham, University of St. Thomas, USA.
(3) M. Y. Dhange, Aliated to Visvesvaraya Technological University, Dr. PG Halakatti College of Engineering and Technology, India.
Complete Peer review History: http://www.sciencedomain.org/review-history/22117

Original Research Article

Received: 2nd November 2017
Accepted: 27th November 2017
Published: 1st December 2017

Abstract

In this paper, the effects of heat generation and MHD on free convection flow along a vertical flat plate have been investigated. Joule heating and heat conduction due to wall thickness *b* are considered in this investigation. The non-dimensional equations are then transformed into non-linear equations by introducing a non- similarity transformation. The resulting equations together with their corresponding boundary conditions are solved numerically by using the finite difference method. Numerical results for the velocity profiles, temperature profiles, skin friction coefficient and the surface temperature distributions are shown both on graphs and tabular form for different values of the parameters.

Keywords: Free convection; Joule heating; magneto-hydrodynamics and heat generation.

**Corresponding author: E-mail: mmparvez@duet.ac.bd;*

1 Introduction

Natural convection heat transfer has gained considerable attention because of its numerous applications in the areas of energy conservations cooling of electrical and electronics components, design of solar collectors, heat exchangers and many others. One common application is the fuse used in electric circuits. It is a short piece of metal, inserted in a circuit, which melts when excessive current flows through it and thus breaks the circuit. It thus protects appliances. The material of a fuse generally has a low melting point and high conductivity. Familiar domestic applications are the electric iron, bread toaster, even electric kettle, heater, etc. The main difficulty in solving natural convection problems lies in the determination of the velocity field, which greatly influences the heat transfer process. El-Amin [1] also studied combined effects of viscous dissipation and Joule heating on MHD forced convection over a non isothermal horizontal cylinder embedded in a fluid saturated porous medium. Gebhart [2] investigated the effects of viscous dissipation in natural flow. Alam et al. [3] studied the effects of pressure stress work and viscous dissipation in natural convection flow along a vertical flat plate with heat conduction. Joule heating effects on the coupling of conduction with magneto-hydrodynamic free convection flow from a vertical flat plate have been investigated by Alim et al. [4]. Combined effect of viscous dissipation and Joule heating on the coupling of conduction and free convection along a vertical flat plate have been investigated by Alim et al. [5]. Vajravelu et al. [6] studied the effects of heat transfer in a viscous fluid over a stretching sheet with viscous dissipation and internal heat generation. Hossain [7] analyzed the viscous and Joule heating effects on MHD free convection flow with variable plate temperature. Hossain et al. [8] investigated the effects of natural convection flow along a vertical wavy surface temperature in presence of heat generation / absorption. Miyamoto et al. [9] has considered the effect of axial heat conduction in a vertical flat plate on free convection heat transfer. Molla et al. [10] have been investigated the effects of magneto-hydrodynamic natural convection flow on a sphere in presence of heat generation. Pozzi and Lupo [11] has shown that the coupling of conduction with laminar natural convection along a flat plate. The present investigation is concerned with the effects of heat generation on the skin friction and the surface temperature distribution in the entire region from upstream to down-stream of a viscous incompressible and electrically conducting fluid from a vertical flat plate in presence of magnetic field. It has been studied that the effect of the magnetic parameter *M,* the Joule heating parameter *Jul*, the Prandtl number *Pr* and the heat generation parameter *Q* on the velocity and temperature fields as well as on the skin friction and surface temperature. In the following sections detailed derivations of the governing equations for the flow are discussed.

2 Governing Equations of the Flow

It has been considered that the steady two dimensional laminar free convection boundary layer flow of a viscous incompressible and electrically conducting fluid along a side of a vertical flat plate of thickness '*b*' insulated on the edges with temperature T_b maintained on the other side in the presence of a uniformly distributed transverse magnetic field has been considered. The flow configuration and the coordinates system are shown in Fig. 1.

The mathematical statement of the basic conservation laws of mass, momentum and energy for the steady viscous incompressible and electrically conducting flow, after simplifying we have

$$\frac{\partial U}{\partial X}+\frac{\partial V}{\partial Y}=0 \tag{1}$$

$$U\frac{\partial U}{\partial X}+V\frac{\partial U}{\partial Y}=\nu\frac{\partial^2 U}{\partial Y^2}+g\beta\left(T-T\infty\right)-\frac{\sigma B_0^2 U}{\rho} \tag{2}$$

$$U\frac{\partial T}{\partial X}+V\frac{\partial T}{\partial Y}=\frac{K}{\rho C_P}\frac{\partial^2 T}{\partial Y^2}+\frac{\sigma B_0^2}{\rho C_P}U^2+\frac{Q_0}{\rho C_P}\left(T-T_\infty\right) \tag{3}$$

Where, U and V are the velocity components along the X and Y axis respectively, T is the temperature of the fluid and T_∞ is the ambient fluid temperature in the boundary layer , g is the acceleration due to gravity, κ is the thermal conductivity, ρ is the density, C_p is the specific heat at constant pressure and ν is the kinematic viscosity of the fluid. The amount of heat generated or absorbed per unit volume is $Q_0(T-T_\infty)$, Q_0 being a constant, which may take either positive or negative. The source term represents the heat generation when $Q_0 > 0$ and the heat absorption when $Q_0 < 0$. In the energy equation heat generation and Joule heating terms are included. Here for exterior conditions we know, $\partial P/\partial X = \rho_e g$ and $\rho = \rho_e$, P is the pressure, B_0 is the magnetic field strength and σ is the electric conductivity.

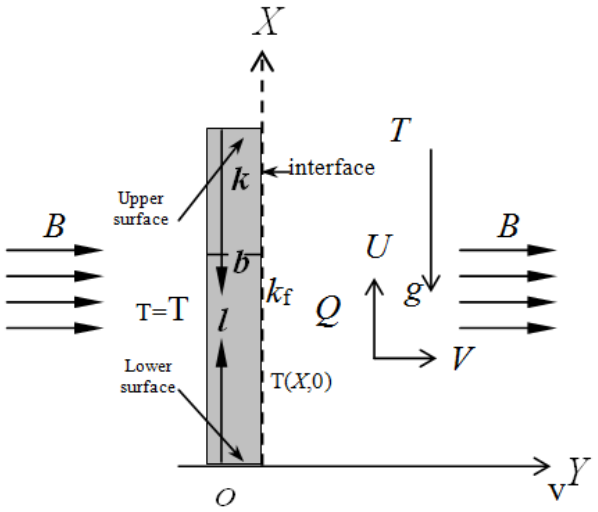

Fig. 1. Physical configuration and coordinates system

The appropriate boundary conditions to be satisfied by the above equations are

$$U = 0,\ V = 0 \text{ at } Y = 0$$
$$U \to 0, T \to T_\infty \text{ as } Y \to \infty \tag{4}$$

The temperature and the heat flux are considered continuous at the interface for the coupled conditions and at the interface we must have

$$\frac{k_s}{k_f}\frac{\partial T_{so}}{\partial Y} = \left(\frac{\partial T}{\partial Y}\right)_{Y=0} \tag{5}$$

Where k_s and k_f are the thermal conductivity of the solid and the fluid respectively. The temperature T_{so} in the solid as given by A. Pozzi and M. Lupo [11] is

$$T_{so} = T(X,0) - \{T_b - T(X,0)\}\frac{Y}{b} \tag{6}$$

Where $T(X,0)$ is the unknown temperature at the interface to be determined from the solutions of the equations.

We observe that the equations (1) - (3) together with the boundary conditions (4) - (5) are non-linear partial differential equations. In the following sections the solution methods of these equations are discussed in details below.

3 Transformation of the Governing Equations

Equations (1) – (3) may now be non-dimensionalized by using the following dimensionless dependent and independent variables:

$$x = \frac{X}{L},\ y = \frac{Y}{L}d^{1/4},\ U = \frac{\nu}{L}d^{1/2}u,\ V = \frac{\nu}{L}d^{1/4}v \tag{7}$$

For the problem of natural convection, its parabolic character has no characteristic length; L has been defined in terms of ν and g, which are the intrinsic properties of the system. The reference length along the 'y' direction has been modified by a factor $d^{1/4}$ in order to eliminate this quantity from the dimensionless equations and the boundary conditions.

The magneto hydrodynamic field in the fluid is governed by the boundary layer equations, which in the non-dimensional form obtained by introducing the dimensionless variables described in (7), may be written as

$$\frac{\partial u}{\partial x} + \frac{\partial v}{\partial y} = 0 \tag{8}$$

$$u\frac{\partial u}{\partial x} + v\frac{\partial u}{\partial y} + Mu = \frac{\partial^2 u}{\partial y^2} + \theta \tag{9}$$

$$u\frac{\partial \theta}{\partial x} + v\frac{\partial \theta}{\partial y} = \frac{1}{p_r}\frac{\partial^2 \theta}{\partial y^2} + u^2 Jul + Q\theta \tag{10}$$

Where $M = \sigma B_0{}^2 L^2 / \mu d^{1/2}$, the dimensionless magnetic parameter, $\Pr = \mu C_p / \kappa_f$, the Prandtl number, $Jul = \sigma B_0^2 \nu d^{1/2} / \rho C_p (T_b - T_\infty)$, the Joule-heating parameter and $Q_0 L^2 / \mu C_P d^{1/2} = Q$ is the heat generation parameter. The corresponding boundary conditions (4) - (6) take the following form:

$$u = v = 0,\ \theta - 1 = p\left(\frac{\partial \theta}{\partial y}\right) \text{ at } y = 0$$
$$u \to o,\ \theta \to 0 \text{ as } y \to \infty \tag{11}$$

Where p is the conjugate conduction parameter given by

$p = \left(\frac{k_f}{k_s}\right)\left(\frac{b}{L}\right)d^{\frac{1}{4}}$. The order of magnitude of 'p' depends actually on b/L, k_f/k_s and $d^{\frac{1}{4}}$ being the order of unity. The term b/L attains values much greater than one because of L being small. In case of air, $\left(\frac{k_f}{k_s}\right)$ becomes very small when the vertical plate is highly conductive i.e. $k_s \rangle\rangle 1$ and for materials, O $\left(\frac{k_f}{k_s}\right)$ = 0.1 such as glass. Therefore in different cases 'p' is different but not always a small number. In the present investigation we have considered p = 1 which is accepted for b/L of O$\left(\frac{k_f}{k_s}\right)$.

To solve the equations (9) – (10) subject to the boundary conditions (1.11), the following transformations were introduced for the flow region starting from upstream to downstream.

$$\psi = x^{4/5}(1+x)^{-1/20} f(x,\eta),\ \eta = yx^{-1/5}(1+x)^{-1/20}, \theta = x^{1/5}(1+x)^{-1/5} h \tag{12}$$

Here η is the dimensionless similarity variable and ψ is the stream function which satisfies the equation of continuity and $u = \frac{\partial \psi}{\partial y}, v = -\frac{\partial \psi}{\partial x}$ and $h(x,\eta)$ is the dimensionless temperature. Therefore, substituting these transformations into equations (9) and (10) and after simplifying, we get the following transformed non-dimensional equations.

$$f''' + \frac{16+15x}{20(1+x)} ff'' - \frac{6+5x}{10(1+x)} f'^2 - Mx^{2/5}(1+x)^{1/10} f' + h = x\left(f' \frac{\partial f'}{\partial x} - f'' \frac{\partial f}{\partial x}\right) \tag{13}$$

$$\frac{1}{P_r} h'' + \frac{16+15x}{20(1+x)} fh' - \frac{1}{5(1+x)} fh + Jul\, x^{\frac{7}{5}}(1+x)^{-\frac{1}{2}} f'^2 + Qx^{1/5}(1+x)^{-1/5} h = x\left(f' \frac{\partial h}{\partial x}\right) - h' \frac{\partial f}{\partial x} \tag{14}$$

In the above equations the primes denote differentiation with respect to η.

The boundary conditions (11) take the following form

$$f(x,0) = f'(x,0) = 0,\ h'(x,0) = -(1+x)^{1/4} \tag{15}$$
$$+x^{1/5}(1+x)^{1/20} h(x,0) f'(x,\infty) = 0, as\ h'(x,\infty) = 0$$

The solutions of the above equations (13) and (14) together with the boundary conditions (15) enable us to calculate the skin friction τ and the surface temperature θ at the surface in the boundary layer from the following relations:

$$\tau = \mu\left\{x^{2/5}\left(1+x\right)^{-3/20} f''\left(x,0\right)\right\} \tag{16}$$

$$\theta = \left\{x^{1/5}\left(1+x\right)^{-1/5} h\left(x,0\right)\right\} \tag{17}$$

4 Method of Solution

This paper concerns the natural convection flow on magneto-hydrodynamics of viscous incompressible fluid along a uniformly heated vertical flat plate in presence of Joule heating and heat generation has been investigated using the very efficient implicit finite difference method known as the Keller box scheme developed by Keller [12], which is well documented by Cebeci and Bradshaw [13].

To apply the aforementioned method, Equations (13) and (14) their boundary conditions (15) are first converted into the following system of first order equations. For this purpose we introduce new dependent variables $u\left(\xi,\eta\right)$, $v\left(\xi,\eta\right)$, $p\left(\xi,\eta\right)$ and $g\left(\xi,\eta\right)$ so that the transformed momentum and energy equations can be written as

$$f' = u \tag{18}$$

$$u' = v \tag{19}$$

$$g' = p \tag{20}$$

$$v' + P_1 f\, u' - P_2 u^2 - P_3 u + g = \xi\left(u\frac{\partial u}{\partial \xi} - v\frac{\partial f}{\partial \xi}\right) \tag{21}$$

$$\frac{1}{\mathrm{Pr}} p' + P_1 f\, p - P_4 u\, g + P_5 u^2 + P_6\, g = \xi\left(u\frac{\partial g}{\partial \xi} - p\frac{\partial f}{\partial \xi}\right) \tag{22}$$

Where $x = \xi$, $h = g$ and $P_1 = \dfrac{16+15x}{20(1+x)}$, $P_2 = \dfrac{6+5x}{10(1+x)}$, $P_3 = Mx^{\frac{2}{5}}(1+x)^{\frac{1}{10}}$,

$P_4 = \dfrac{1}{5(1+x)}$, $P_5 = Jul\, x^{\frac{7}{5}}(1+x)^{-\frac{1}{2}}$, $P_6 = Q\, x^{\frac{1}{5}}(1+x)^{-\frac{1}{5}}$

and the boundary conditions (15) are

$$\begin{aligned} &f\left(\xi,0\right) = 0, \quad u\left(\xi,0\right) = 0, g\left(\xi,0\right) = -\left(1+\xi\right)^{\frac{1}{4}} + \xi^{\frac{1}{5}}\left(1+\xi\right)^{\frac{1}{20}} g\left(\xi,0\right) \\ &u\left(\xi,\infty\right) = 0, \quad p\left(\xi,\infty\right) = 0 \end{aligned} \tag{23}$$

Now consider the net rectangle on the (ξ, η) plane shown in the Fig. 2 and denote the net points by

$$\xi^0 = 0, \xi^n = \xi^{n-1} + k_n, n = 1,2,3,---,N \text{ and } \eta_0 = 0, \eta_j = \eta_{j-1} + h_j, j = 1,2,3,---,J \quad (24)$$

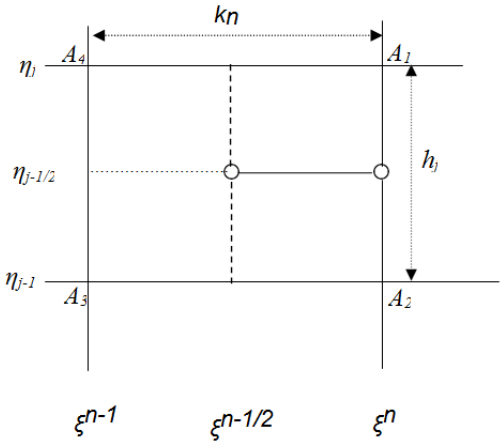

Fig. 2. Net rectangle of difference approximations for the Box scheme

Here n and j are just sequence of numbers on the (ξ, η) plane, k_n and h_j are the variable mesh widths. Approximate the quantities *f*, *u*, *v* and *p* , at the points (ξ^n, η_j) of the net by f_j^n, u_j^n, v_j^n, p_j^n which call net function. It is also employed that the notation P_j^n for the quantities midways between net points shown in Fig. 2 and for any net functions as

$$\xi^{n-\frac{1}{2}} = \frac{1}{2}\left(\xi^n + \xi^{n-1}\right) \quad (25)$$

$$\eta_{j-\frac{1}{2}} = \frac{1}{2}\left(\eta_j + \eta_{j-\frac{1}{2}}\right) \quad (26)$$

$$g_j^{n-\frac{1}{2}} = \frac{1}{2}\left(g_j^n + g_j^{n-1}\right) \quad (27)$$

$$g_{j-\frac{1}{2}}^n = \frac{1}{2}\left(g_j^n + g_{j-1}^n\right) \quad (28)$$

The finite difference approximation according to box method to the three first order ordinary differential equation (18)-(20) are written for the mid - point $\left(\xi^n, \eta_{j-\frac{1}{2}}\right)$ of the segment A_1A_2 shown in Fig. 2.

$$\frac{f_j^n - f_{j-1}^n}{h_j} = u_{j-\frac{1}{2}}^n = \frac{u_{j-1}^n + u_j^n}{2} \quad (29)$$

$$\frac{u_j^n - u_{j-1}^n}{h_j} = v_{j-\frac{1}{2}}^n = \frac{v_j^n + v_{j-1}^n}{2} \tag{30}$$

$$\frac{g_j^n - g_{j-1}^n}{h_j} = p_{j-\frac{1}{2}}^n = \frac{p_j^n + p_{j-1}^n}{2} \tag{31}$$

The finite difference approximation to the first order differential equation (21) and (22) are written for the mid - point $\left(\xi^{n-\frac{1}{2}}, \eta_{j-\frac{1}{2}}\right)$ of the rectangle $A_1A_2A_3A_4$. This procedure yields

$$\begin{aligned}&\frac{1}{2}\left(\frac{v_j^n - v_{j-1}^n}{h_j}\right) + \frac{1}{2}\left(\frac{v_j^{n-1} - v_{j-1}^{n-1}}{h_j}\right) + \left(P_1 f\ v\right)_{j-\frac{1}{2}}^{n-\frac{1}{2}} - \left(P_2 u^2\right)_{j-\frac{1}{2}}^{n-1} - \left(P_3 u\right)_{j-\frac{1}{2}}^{n-1} + g_{j-\frac{1}{2}}^{n-1} \\ &= \xi_{j-\frac{1}{2}}^{n-\frac{1}{2}}\left(u_{j-\frac{1}{2}}^{n-\frac{1}{2}} \frac{u_{j-\frac{1}{2}}^n - u_{j-\frac{1}{2}}^{n-1}}{k_n} - v_{j-\frac{1}{2}}^{n-\frac{1}{2}} \frac{f_{j-\frac{1}{2}}^n - f_{j-\frac{1}{2}}^{n-1}}{k_n}\right)\end{aligned} \tag{32}$$

$$\begin{aligned}&\frac{1}{2\,\mathrm{Pr}}\left(\frac{p_j^n - p_{j-1}^n}{h_j}\right) + \frac{1}{2\,\mathrm{Pr}}\left(\frac{p_j^{n-1} - p_{j-1}^{n-1}}{h_j}\right) + \left(P_1 f\ p\right)_{j-\frac{1}{2}}^{n-\frac{1}{2}} - \left(P_4 ug\right)_{j-\frac{1}{2}}^{n-\frac{1}{2}} + \left(P_5\, u^2\right)_{j-\frac{1}{2}}^{n-\frac{1}{2}} \left(P_6\, g\right)_{j-\frac{1}{2}}^{n-\frac{1}{2}} \\ &= \xi_{j-\frac{1}{2}}^{n-\frac{1}{2}}\left(u_{j-\frac{1}{2}}^{n-\frac{1}{2}} \frac{g_{j-\frac{1}{2}}^n - g_{j-\frac{1}{2}}^{n-1}}{k_n} - p_{j-\frac{1}{2}}^{n-\frac{1}{2}} \frac{f_{j-\frac{1}{2}}^n - f_{j-\frac{1}{2}}^{n-1}}{k_n}\right)\end{aligned} \tag{33}$$

The above equations are to be linearized by using Newton's Quasi-linearization method. Then linear algebraic equations can be written in block matrix which form a coefficient matrix. The whole procedure, namely reduction to first order followed by central difference approximations, Newton's Quasi-linearization method and the block Thomas algorithm, is well known as the Keller-box method.

5 Results and Discussion

Here we have investigated the problem of the steady two dimensional laminar free convection boundary layer flow of a viscous incompressible and electrically conducting fluid along a side of a vertical flat plate of thickness '*b*' insulated on the edges with temperature T_b maintained on the other side in the presence of a uniformly distributed transverse magnetic field and heat generation. Solutions are obtained for the fluid having Prandtl number *Pr* = 0.01, 0.10 0.50, 0.73, 1.00 and for a wide range of the Joule heating parameter *Jul* = 0.20, 0.40, 0.70, 0.90, the magnetic parameter *M* = 1.10, 1.40, 1.60, 1.80 and the heat generation parameter *Q* = 0.20, 0.40, 0.70, 0.90. $f\left(x,\eta\right)$, $h\left(x,\eta\right)$.

Fig. 3(a) and 3(b) represent, respectively, the velocity and the temperature profiles for different values of the Joule heating parameter *Jul* for particular values of the Prandtl number *Pr*=0.72, the magnetic parameter *M*=1.00 and the heat generation parameter *Q*=0.20. We observe from Fig. 3(a), that an increase in the Joule heating parameter *Jul*, is associated with a considerable increase in velocity profiles but near the surface of the plate the velocity increases and become maximum and then decreases and finally approaches to zero asymptotically. However Fig. 3(b) shows the distribution of the temperature profiles against η for some values of the Joule heating parameter *Jul* (=0.90, 0.70, 0.40, 0.20). Clearly it is seen that the temperature distribution increases owing to increasing values of the Joule heating parameter *Jul* and the maximum is at the adjacent of the plate wall. The local maximum values of the temperature profiles are 1.7662, 1.6886, 1.6164, 1.5496 for *Jul* = 0.90, 0.70, 0.50, 0.30 respectively and each of which attains at the surface. Thus the temperature profiles increase by 13.98% as *Jul* increases from 0.30 to 0.90.

Figs. 4(a)-4(b) display results for the velocity and temperature profiles, for different small values of magnetic parameter M (=1.10, 1.40, 1.60, 1.80, 2.10) plotted against η at Pr = 0.72, Jul=0.50 and Q = 0.60. It is seen from Fig. 4(a) that the velocity profile is influenced considerably and decreases when the value of magnetic parameter M increases. But near the surface of the plate velocity increases significantly and then decreases slowly and finally approaches to zero. Also, it has been observed that the temperature field increases for increasing values of magnetic parameter M in Fig. 4(b). Fig. 5(a)-5(b) display results for the velocity and temperature profiles, for different small values of heat generation parameter Q (=0.20, 0.40, 0.70, 0.90) plotted against η at Pr = 0.72, M = 0.50 and Jul = 0. Also Fig. 5(b), it has been observed that when value of heat generation parameter Q increases, the temperature distribution also increases significantly.

Fig. 6(a)-6(b) display results for the velocity and temperature profiles, for different small values of Prandtl number Pr (=1.00, 0.73, 0.40, 0.20) plotted against η at M = 0.90, Jul=0.70 and Q = 0.50. It is seen from Fig. 6(a) that the velocity profile is influenced considerably and decreases when the value of magnetic parameter Pr increases.

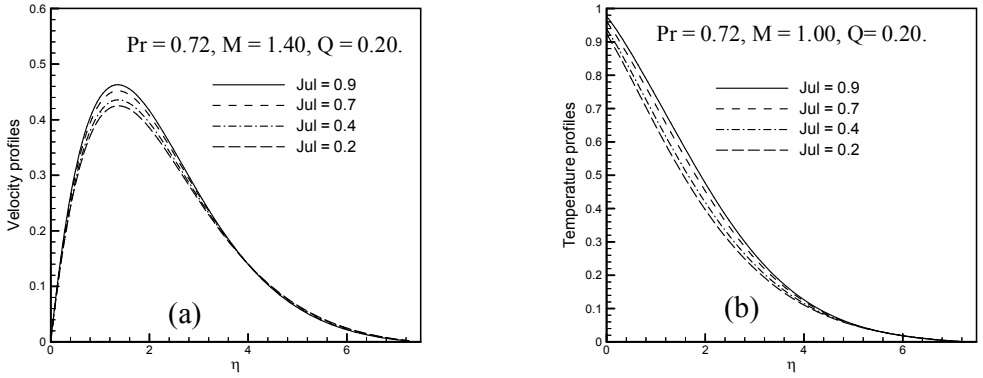

Fig. 3(a) and Fig. 3(b). Variation of dimensionless velocity profiles $f'(x,\eta)$ and temperature profiles against dimensionless distance η for different values of Joule heating parameters Jul with Pr = 0.72, M = 1.40 and Q = 0 .20

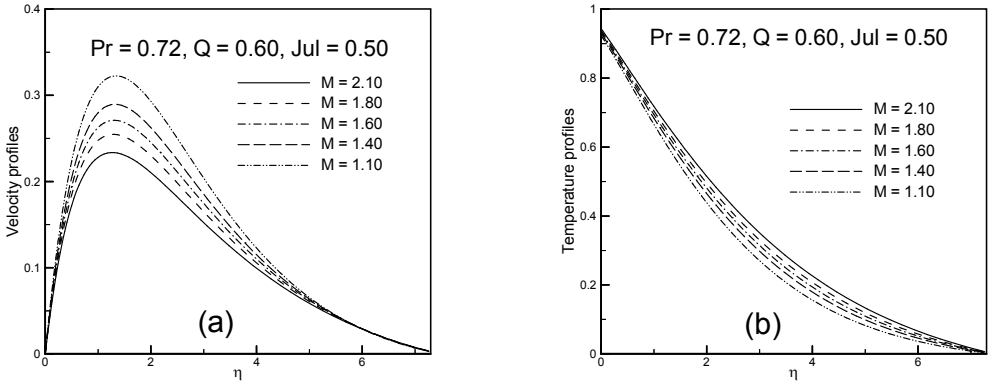

Fig. 4(a) and Fig. 4(b). Variation of dimensionless velocity profiles $f'(x,\eta)$ and temperature profiles against dimensionless distance η for different values of Magnetic parameters Jul with Pr = 0.72, Jul = 0.50 and Q = 0 .60

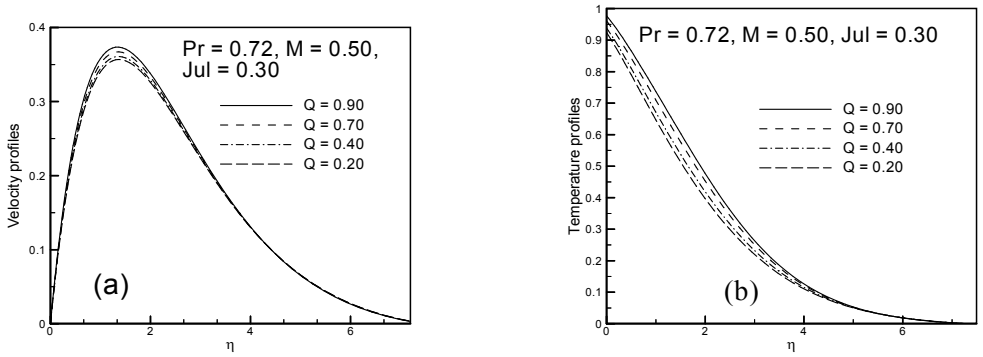

Fig. 5(*a*) and Fig. 5(b). Variation of dimensionless velocity profiles $f'(x,\eta)$ and temperature profiles against dimensionless distance η for different values of heat generation parameters Q with $Pr = 0.72$, $M = 0.50$ and $Jul = 0.30$

But near the surface of the plate velocity increases significantly and then decreases slowly and finally approaches to zero. Also, it has been observed that the temperature field decreases for increasing values of Prandtl number *Pr* in Fig. 6(b).

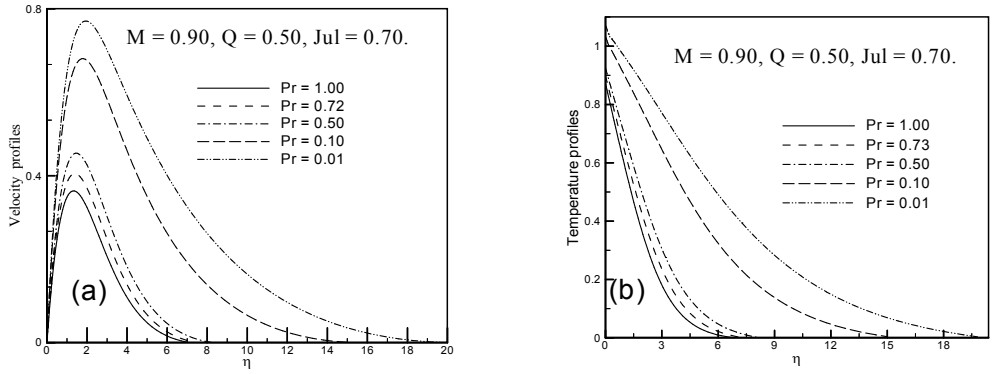

Fig. 6(*a*) and Fig. 6(b). Variation of dimensionless velocity profiles $f'(x,\eta)$ and temperature profiles against dimensionless distance η for different values of Prandtl number parameters Q with $Pr = 0.72$, $M = 0.50$ and $Jul = 0.30$

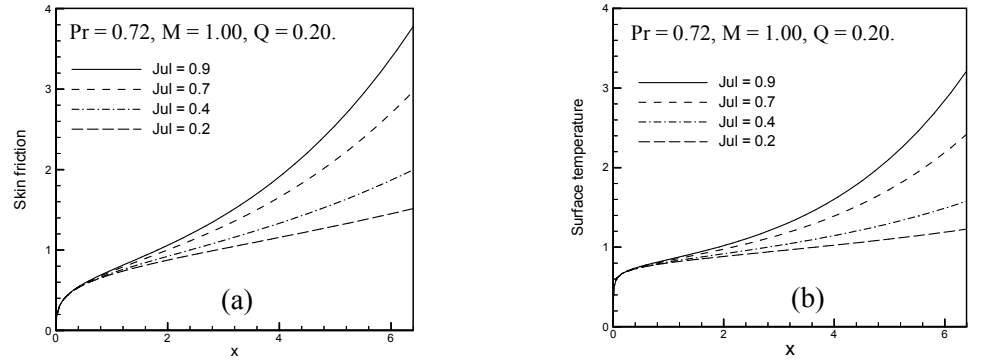

Fig. 7(*a*) and Fig. 7(b). Variation of skin friction coefficient $f''(x, 0)$ and surface temperature $\theta(x, 0)$ with dimensionless distance x for different values of Joule heating parameters Jul with $Pr = 0.72$, $M = 1.40$ and $Q = 0.20$

Numerical values of the velocity gradient $f''(x,0)$ and the surface temperature $\theta(x,0)$ are depicted graphically in Fig. 7(a) and 7(b) respectively against the axial distance x in the interval [0, 6.5] x for different values of Joule heating parameter *Jul* (= 0.90, 0.70, 0.40, 0.20). It is seen from Fig. 7(a) that the skin-friction $f''(x,0)$ increases when the Joule heating parameter, *Jul* increases. It is also observed in Fig. 7(b) that the surface temperature $\theta(x,0)$ distribution increases while *Jul* increases.

The effect of magnetic parameter M (= 2.10, 1.80, 1.60, 1.40, 1.10) on the skin-friction $f''(x,0)$ and the surface temperature distribution $\theta(x,0)$ against x for Pr = 0.72, Jul = 0.50, and Q = 0.60 is shown in Fig. 8(a) - 8 (b). It is found that the values of the skin-friction $f''(x,0)$ and the surface temperature distribution $\theta(x,0)$ both decrease for increasing values of magnetic parameter M. Also, it is observed that the values of the skin-friction $f''(x,0)$ decrease by 95.73% and the surface temperature distribution $\theta(x,0)$ decreases by 97.26% while M increases from 1.10 to 2.10.

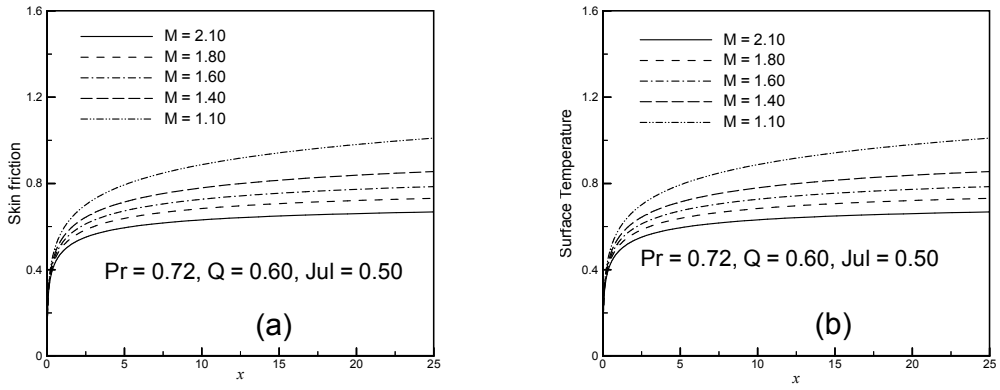

Fig. 8(*a*) and Fig. 8(b). Variation of skin friction coefficient $f''(x, 0)$ and surface temperature $\theta(x, 0)$ with dimensionless distance x for different values of Magnetic parameters with Pr = 0.72, Jul = 0.50 and Q = 0 .60

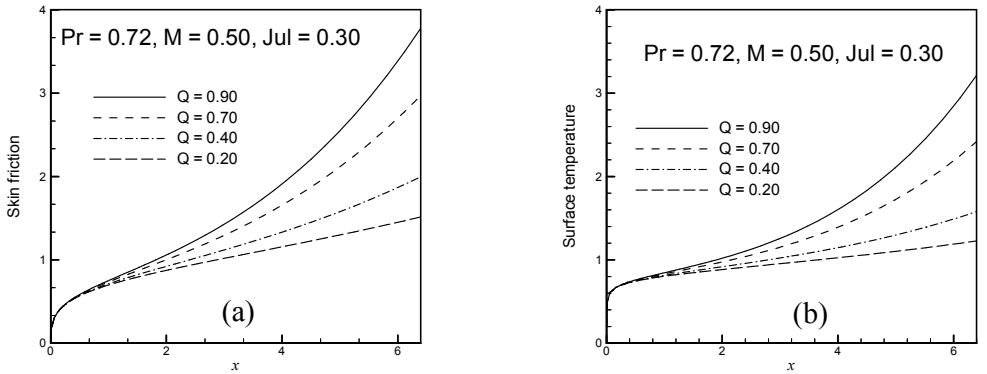

Fig. 9(*a*) and Fig. 9(b). Variation of skin friction coefficient $f''(x, 0)$ and surface temperature $\theta(x, 0)$ with dimensionless distance x for different values of heat generation parameters Q with Pr = 0.72, M = 0.50 and Jul = 0 .30

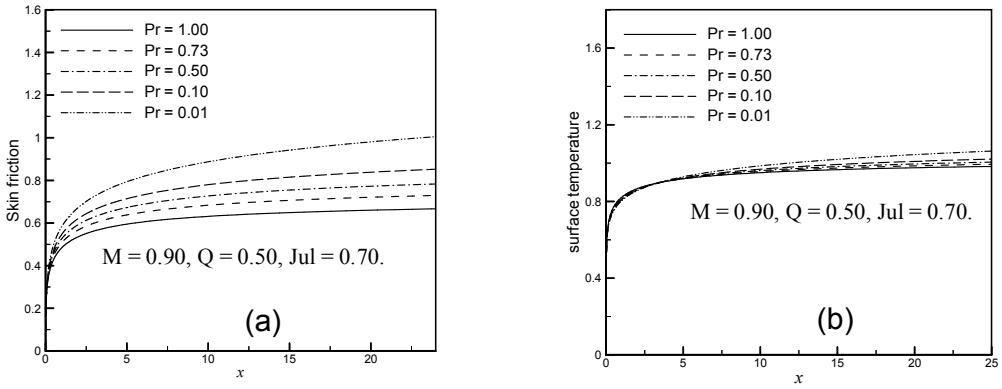

Fig. 10(*a*) and Fig. 10(b). Variation of skin friction coefficient $f''(x, 0)$ and surface temperature $\theta(x, 0)$ with dimensionless distance x for different values of Prandtl number parameters Q with $Pr = 0.72$, $M = 0.50$ and $Jul = 0.30$

Fig. 8(a)-8(b) illustrate the variation of skin-friction $f''(x,0)$ and surface temperature distribution $\theta(x,0)$ against x for different values of heat generation parameter Q (=0.90, 0.70, 0.40, 0.20). It is seen from Fig. 8(a) that the skin-friction $f''(x,0)$ increases when the heat generation parameter Q increases. It is also observed in Fig. 8(b) that the surface temperature $\theta(x,0)$ distribution increases while Q increases.

In Fig. 9(a), the shear stress coefficient $f''(x,0)$ and Fig. 9(b), the surface temperature $\theta(x,0)$ are shown graphically for different values of the Prandtl number Pr (=0.01, 0.10, 0.50, 0.73, 1.00) when other values of the controlling parameter (M = 0.90, Jul = 0.70, and Q = 0.50). Five values 0.01, 0.10, 0.50, 0.73, 1.00 are taken for Pr, the Prandtl number, 0.73 represents air, 1.00 corresponds to electrolyte solutions such as salt water, 0.01, 0.10 and 0.50 have been used theoretically. Here, it is founded that the skin friction and the surface temperature both decrease for increasing values of Prandtl number.

Table 1. Skin friction coefficient and surface temperature distribution for different values of heat generation parameter Q against x with other controlling parameters $Pr = 0.72$, $Jul = 0.30$, $M = 0.50$

x	$Q = 0.20$		$Q = 0.40$		$Q = 0.70$		$Q = 0.90$	
	$f''(x, 0)$	$\theta(x, 0)$	$f''(x, 0)$	$\theta(x, 0)$	$f''(x, 0)$	$\theta(x, 0)$	$f''(x, 0)$	$\theta(x, 0)$
0.0000	0.0155	0.2052	0.0155	0.2052	0.0155	0.2052	0.0155	0.2052
0.3045	0.5083	0.7352	0.5801	0.8126	0.6663	0.9106	0.7686	1.0338
0.7090	0.6416	0.7907	0.7502	0.8847	0.8851	1.0087	1.0490	1.1701
1.0265	0.7067	0.8152	0.8356	0.9168	0.9982	1.0531	1.1981	1.2332
2.0369	0.8372	0.8614	1.0113	0.9773	1.2373	1.1381	1.5208	1.3559
3.0049	0.9169	0.8885	1.1213	1.0131	1.3913	1.1893	1.7337	1.4311
4.0219	0.9794	0.9095	1.2093	1.0414	1.5169	1.2304	1.9101	1.4924
5.0387	1.0296	0.9263	1.2811	1.0645	1.6211	1.2648	2.0583	1.5443
6.0502	1.0717	0.9405	1.3423	1.0844	1.7111	1.2949	2.1877	1.5903

In Table 1 skin friction coefficient and surface temperature distribution for different values of heat generation Q while M = 0.50, Jul = 0.30 and Pr = 0.72 are entered. Here it is found that the values of skin friction decrease at different position of x for heat generation parameter Q =0.20, 0.40, 0.70, 0.90. The rate of the skin friction increases by 89.08% as the heat generation parameter Q changes from 0.20 to 0.90 at position x = 3.0049. Furthermore, it is seen that the numerical values of the surface temperature distribution

increase for increasing values of heat generation parameter Q. The rate of increase of surface temperature distribution is 61.07% at position $x = 3.0049$ as the heat generation parameter changes from 0.20 to 0.90.

6 Conclusions

The effect of magnetic parameter M, Joule heating parameter Jul, the heat generation parameter Q and the Prandtl number Pr on the magneto-hydrodynamic (MHD) natural convection boundary layer flow along a vertical flat plate has been studied introducing a new class of transformations. The transformed non-similar boundary layer equations governing the flow together with the boundary conditions based on conduction and convection were solved numerically using the very efficient implicit finite difference method together with Keller box scheme. From the present investigation, the following conclusions may be drawn:

- The skin friction coefficient, the surface temperature, the velocity and the temperature profiles increase for the increasing values of the Joule heating parameter Jul.
- The skin friction coefficient, the surface temperature, the velocity and the temperature profiles are increasing for the increasing values of the heat generation parameter Q.
- It has been observed that the skin friction coefficient, the surface temperature distribution, the velocity profile decreases over the whole boundary layer with the increase of the Prandtl number Pr. But the temperature profile increases at some distance against η and then it stars to decrease over the whole boundary layer with the increase of the Prandtl number Pr.
- The effect of magnetic parameter M is to decrease the skin friction coefficient, the surface temperature distribution and the velocity distribution over the whole boundary layer, but reverse case happens for temperature distributions.

Competing Interests

Authors have declared that no competing interests exist.

References

[1] El-Amin MF. Combined effect of viscous dissipation and Joule heating on MHD forced convection over a non isothermal horizontal cylinder embedded in a fluid saturated porous medium. Journal of Magnetism and Magnetic Materials. 2003;263:337-343.

[2] Gebhart B. Effects of viscous dissipation in natural convection. J. of Fluid Mech. 1962;14:225-232.

[3] Alam Md. M, Alim MA, Chowdhury Md. MK. Effect of pressure stress work and viscous dissipation in natural convection flow along a vertical flat plate with heat conduction. Jounal of Naval Architecture and Marine Engineering. 2006;3(2):69-76.

[4] Alim MA, Md. M. Alam, Abdullah-Al-Mamun. Joule heating effect on the coupling of conduction with magneto-hydrodynamic free convection flow from a vertical flat plate. Nonlinear Analysis: Modelling and Control. 2007;12(3):307-316.

[5] Alim MA, Md. M. Alam, Abdullah-Al-Mamun, Belal Hossain. Combined effect of viscous dissipation and Joule heating on the coupling of conduction and free convection along a vertical flat plate. International Communication of Heat and Mass Transfer. 2008;35:338-346.

[6] Vajravelu K, Hadjinicolaou A. Heat transfer in a viscous fluid over a stretching sheet with viscous dissipation and internal heat generation. Int. Comm. Heat Mass Transfer. 1993;20:417-430.

[7] Hossain MA. Viscous and Joule heating effects on MHD free convection flow with variable plate temperature. Int. J. Heat and Mass Transfer. 1992;35(2):3485-3487.

[8] Hossain MA, Molla MM, Yao LS. Natural convection flow along a vertical wavy surface temperature in presence of heat generation / absorption. Int. J. Thermal Science. 2004;43:157-163.

[9] Miyamoto M, Sumikawa J, Akiyoshi T, Nakamura T. Effect of axial heat conduction in a vertical flat plate on free convection heat transfer. Int. J. Heat Mass Transfer. 1980;23:1545-1533.

[10] Molla MM, Taher MA, Chowdhury MMK, Hossain MA. Magneto -hydrodynamic natural convection flow on a sphere in presence of heat generation. Nonlinear Analysis: Modelling and Control. 2005; 10(4):349-363.

[11] Pozzi A, Lupo M. The coupling of conduction with laminar natural convection along a flat plate. Int. J. Heat Mass Transfer. 1988;31(9):1807-1814.

[12] Keller HB. Numerical methods in boundary layer theory. Annual Rev. Fluid Mech. 1978;10:417-443.

[13] Cebeci T, Bradshaw P. Physical and computational aspects of convective heat transfer. Spring, New York; 1984.

Peer-review history:
The peer review history for this paper can be accessed here (Please copy paste the total link in your browser address bar)
http://sciencedomain.org/review-history/22117